Silicon-Doped Hydroxyapatite

A.J. Ruys*

* Senior Research Associate
Centre for Biomedical Engineering
University of New South Wales

Abstract

The role of many ions in biological systems is not fully understood owing to difficulties in microdetermination. Silicon is known to be essential in many biological processes, including skeletal development. Some evidence indicates that silicon acts as a calcifying agent rather than as a resident structural species. This suggests that silicon may be used for enhancement of bone ingrowth rates for bioactive prosthetic materials. Of particular interest is hydroxyapatite $Ca_{10}(PO_4)_6(OH)_2$ [HAp], which has a relatively low bioactivity. The purpose of the present work was to determine the feasibility of chemically doping HAp with silicon. This route is practical because apatites are well known for undergoing extensive isomorphous substitution at all of the cation lattice positions.

HAp was synthesised by the metathesis method using $Ca_3(NO_3)_2$, $(NH_4)_2HPO_4$, and NH_4OH. Silicon was added by a sol-gel route using tetraethyl orthosilicate [TEOS] and ethanol. Silicon was added at levels up to a Si:HAp molar ratio of 50, although most work was done at <2. The samples were sintered at 1100°C for 1 h in air. Characterisation consisted only of X-ray diffraction for semiquantitative phase analysis and lattice parameter determination.

At all silicon levels, $Ca_{10}(PO_4)_4(SiO_4)_2$ formed. At low silicon levels, β-$Ca_3(PO_4)_2$ [β-TCP] formed, while high silicon levels favoured α-$Ca_3(PO_4)_2$ [α-TCP]. A Si-P-O glass also formed at high silicon levels. Lattice parameter measurements indicated that silicon dissolved in the HAp structure up to a Si:HAp molar ratio of ~ 0.36. Ionic radii considerations suggest that the most likely substitution site was that of phosphorus. Charge compensation requires substitution of P^{5+} by Si^{4+} to form holes on the OH^- sites. If so, then the saturated silicon-substituted phase would have the formula $Ca_{10}(P_{1-X}Si_XO_4)_6(OH)_{2-6X}$, where $X = 0.06$, or $Ca_{10}(P_{1-X}Si_XO_4)_6(OH)_2^{6X-}$ in the absence of charge compensation.

Consequently, it is possible to dope HAp with silicon using a sol-gel route. Si:HAp and Si:P molar ratios $\leq 0.36:1$ and $\leq 0.06:0.94$, respectively, should be used in order to avoid formation of biodegradable TCP.

INTRODUCTION

Silicon and Bone Growth

The role of silicon in biological systems is not yet fully understood since microdetermination of silicon in biological systems is very difficult [1]. However, silicon is now known to be essential for the growth and development of vertebrates, being involved in cell wall formation, cross-linking in connective tissues, nucleic acid synthesis, photosynthesis, and other biological processes, particularly with regard to ageing [2,3]. Silicon also has been found to perform a vital role in skeletal development. It is a constituent of collagen [4], and silicon deprivation has been found to retard bone development in chicks [5].

Although the importance of silicon in bone matrix is now well established, its importance in bone mineral is not yet fully understood [1,5,6]. Dietary silicon has been found to increase the rate of bone calcification independent of vitamin D, and nodular ill-formed bone results from silicon deficiency [2]. Silicon has been localised in immature bone by both ion and electron microprobe studies [6,7].

Figure 1 shows an electron microprobe scan of calcium and silicon concentration across a bone mineralising front [6]. While phosphorous distribution is diffuse in calcifying regions [7], this scan revealed the calcium distribution to be preferentially localised to regions of mature bone, as expected, but the silicon distribution was quite the opposite [6]. The scan detected negligible silicon levels in the calcium-rich (mature bone) region and a maximum silicon level of ~0.5 wt% in the calcium-deficient area – the region of active calcification. The figure of ~0.5 wt% was a semiquantitative value since precise determination of the silicon level at a mineralisation site is difficult because these sites are localised and difficult to measure directly. A calcium level of only ~2 wt% was detected in the silicon-rich region. This corresponded to a Ca:P ratio that was too low to form any of the known calcium phosphate phases, and so it was suggested by Carlisle [6] that the bone precursor must be an organic phase containing silicon. Silicon also was found in the metaphyseal blood vessels. These findings suggest that silicon is a calcifying agent rather than a resident structural species.

As further evidence of the role of silicon as a calcification initiator or promoter, the nucleation and growth of bone mineral (hydroxyapatite crystals) have been found to be greatly enhanced on silicon-rich substrates, including SiO_2 [8,9], SiO_2-rich bioglass surfaces [10,11], and polysilicic acid [8].

If silicon is a calcifying agent, this offers the possibility of the use of silicon for the enhancement of bone ingrowth rates for bioactive prosthetic materials. There are only two prosthetic materials that are known to combine the desirable properties of biocompatibility, low to negligible resorption rates *in-vivo*, and the ability to bond chemically with bone. These are hydroxyapatite $Ca_{10}(PO_4)_6(OH)_2$ [HAp] and certain bioactive glass compositions. The bioactivities of these glass formulations are considerably higher than that of HAp [12]. Table 1 summarises the bioactivities of some of the important bioactive glasses and HAp. The bioactivity of these SiO_2-rich glass formulations has been found to be related to the formation of a SiO_2-rich surface layer, with bone-glass chemical bonding following three stages [10]:

1. A silica-rich layer develops on the glass surface, with corresponding linear weight loss from the implant.
2. A thin film of HAp crystals is deposited on the silica-rich layer.
3. The rate of weight loss from the implant declines to the point of no further change.

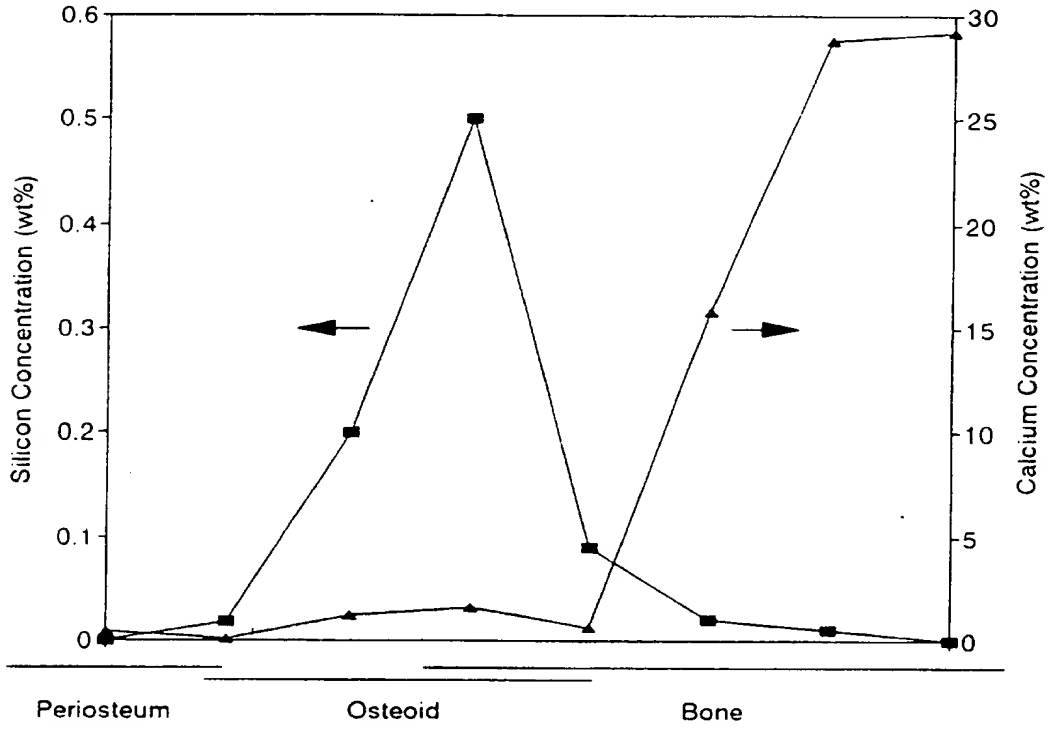

FIGURE 1. ELECTRON MICROPROBE SCANS OF SILICON AND CALCIUM ACROSS A BONE MINERALISING FRONT IN YOUNG RAT TIBIA [6].

TABLE 1. BIOACTIVITIES OF GLASS-BASED MATERIALS AND HYDROXYAPATITE [12].

Bioactive Material	System or Compound	Wt % SiO_2	Peak Bioactivity
45S5-Bioglass	Na_2O-CaO-P_2O_5-SiO_2	45	~ 15 days
KGS-Ceravital	$Ca(PO_3)_2$-Na_2O-CaO-SiO_2	46	~ 45 days
A-W Glass-Ceramic	$Ca_{10}(PO_4)_6(O,F)_2$-CaO-MgO-SiO_2	45	~ 100 days
Hydroxyapatite	$Ca_{10}(PO_4)_6(OH)_2$	--	~ 110 days

Since silicon may enhance the bioactivity of these glass-based materials, the relatively low bioactivity of HAp may be due to the absence of silicon from its structure. However, since A-W glass-ceramic has a peak bioactivity of the same scale as HAp, there is some question as to this suggestion. The purpose of the present work was to address the potential benefits and problems involved in the silicon doping of HAp, since HAp has the advantage over bioactive glasses and glass-ceramics of being chemically similar to bone mineral.

Silicon in Hydroxyapatite

It is well known that the bone ingrowth capacity of HAp can be enhanced only by increasing the porosity, but the low strength of porous HAp limits its use to monolithic implants in nonload-bearing sites or bioactive coatings. If silicon is a bone calcifying agent [6], it may be possible to enhance the bone ingrowth rate of dense HAp by silicon impregnation, thereby increasing the bioactivity without compromising strength. Silicon doping of HAp is known to occur in geological systems since apatites are capable of undergoing extensive isomorphous substitution [13]. The existence of naturally occurring calcium silicophosphate apatite minerals has been documented in various studies.

Apatites have a hexagonal crystal structure [14]. Molecular models of fluorapatite are shown in Figures 2 and 3. The fluorapatite structure represents the generalised apatite formula range [13]:

$$A_{10}(XO_4)_6Z_2 - A_9(XO_4)_6$$

In the case of HAp, with the formula $Ca_{10}(PO_4)_6(OH)_2$, calcium, phosphorous, and hydroxyl groups occupy the *A*, *X*, and *Z* sites, respectively. Isomorphous substitution at each of these sites is governed by the upper and lower ionic radii limits, as listed by Cockbain [13]:

A site	0.069 – 0.174 nm
X site	0.026 – 0.056 nm
Z site	0.131 – 0.216 nm

The *Z* sites are large channels parallel to the *c* axis, analogous to the channels in a zeolite, so they can be vacant. Thus, the occupants of the *Z* site are weakly held, and many apatites, such as tricalcium phosphate β-$Ca_3(PO_4)_2$ [β-TCP], have empty *Z* sites [13].

The present work involved the development of techniques for the doping of HAp by silicon and subsequent investigation of the effects of silicon on the crystal structure of HAp, with the aim of establishing whether or not such a material would be suited to clinical trials.

Methods and Materials

HAp Synthesis

The HAp used in the present work was synthesised by the metathesis method of Jarcho *et al.* [15]. The manufacturer's specifications of the $Ca_3(NO_3)_2$, $(NH_4)_2HPO_4$, and NH_4OH used in the synthesis are compiled in Table 2. The $Ca_3(PO_4)_2$ precipitate was simultaneously stirred and boiled. The stir/boil method was necessary in order to eliminate TCP from the calcined product. This could not be achieved reliably with cold-stirring for the recommended time of 24 h nor for longer periods up to 48 h. The resulting precipitates of ~20 nm diameter (assumed size [15]) HAp crystallites were washed twice to remove the NH_4NO_3 by filtering through a Büchner funnel and resuspending in demineralised water by means of high-speed stirring. After the second washing, the wet filter cake was resuspended in ethanol in preparation for the silicon addition process. The filter cake was not allowed to dry between the final washing stage and resuspension in ethanol in order to prevent aggregation.

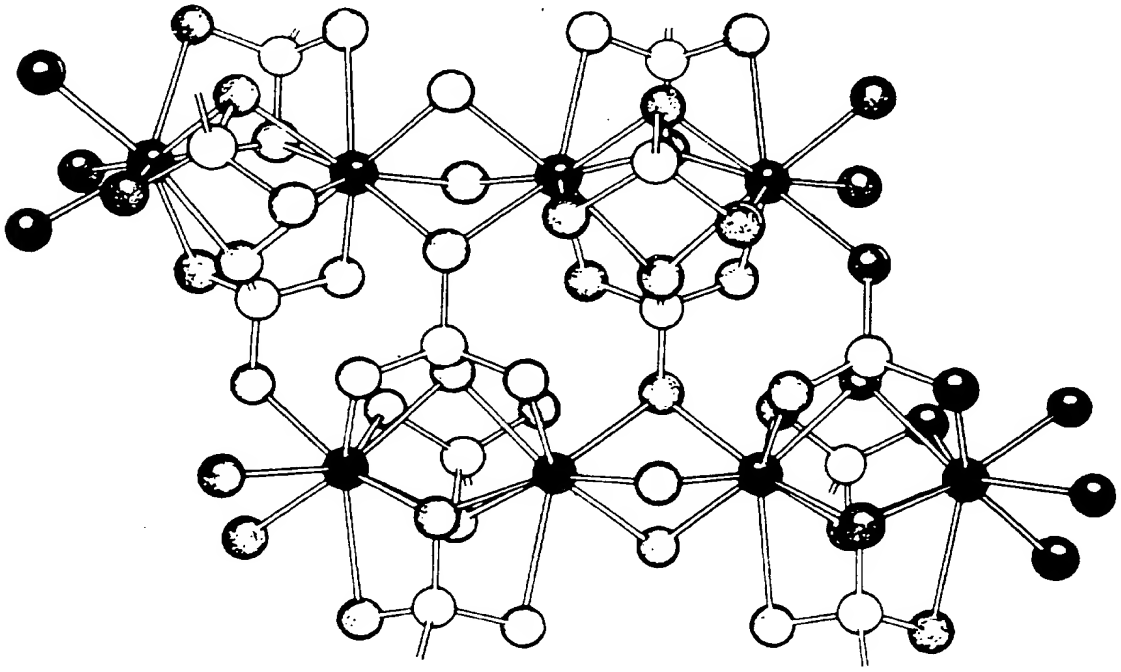

FIGURE 2. FLUORAPATITE STRUCTURE WITH *C* AXIS ORIENTED HORIZONTALLY WITHIN PAGE (BLACK = CA, WHITE = P, GREY = O) [11].

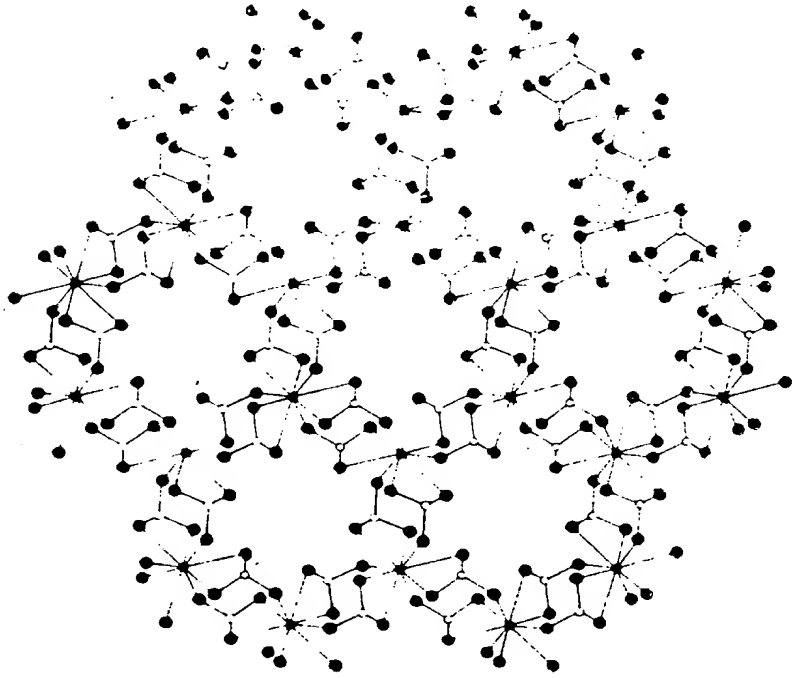

FIGURE 3. FLUORAPATITE STRUCTURE WITH *C* AXIS ORIENTED NORMAL TO PAGE (BLACK = CA, WHITE = P, GREY = O) [11].

TABLE 2. RAW MATERIALS.

Material	Purity	Supplier
$Ca_3(NO_3)_2$	98.5 wt%	Ajax Chemicals
$(NH_4)_2HPO_4$	98.0 wt%	Ajax Chemicals
NH_4OH	99.4 wt%	Ajax Chemicals
$(C_2H_5)_4SiO_4$	99.0 wt%*	Union Carbide
C_2H_5OH	95.8 vol%	CSR Chemical
Al	99.5 wt%	Cerac Inc.

* Minimum

Silicon Additions

A sol-gel method was used to dope the HAp with silicon. This method utilised tetraethyl orthosilicate (TEOS), which decomposes into ethanol and colloidal silica in the presence of water in accordance with the reaction:

$$(C_2H_5)_4SiO_4 + 2H_2O \longrightarrow 4C_2H_5OH + SiO_2$$

A solution of TEOS was added in measured amounts by burette to the HAp/ethanol suspension, and the suspension was subjected to high-speed stirring for 10 min. Excess water then was added to hydrolyse the ethyl silicate, followed by another high-speed stirring for 10 min. After this, the ethanol was removed by evaporation. The resulting filter cake then was crushed and pelletised at 200 MPa into 12.5 mm ∅ x 2.5 mm thickness samples. These pellets were sintered at 1100°C for 1 h in air, using a heating rate of 60°C/h.

Silicon addition levels were defined as atoms of silicon per HAp unit cell, which is the Si:HAp molar ratio:

$$\text{Si:HAp} = \frac{\text{Moles } SiO_2}{\text{Moles } Ca_{10}(PO_4)_6(OH)_2}$$

The silicon addition level was varied from 0 to 50, with the majority of the samples being below 2.

Sample Characterisation

For each sample, the semiquantitative phase composition and the lattice parameters of the HAp phase of the samples were measured by X-ray powder diffraction (Philips, Type PW 1140/00 powder diffractometer) using CuKα radiation. Powdered aluminium was used as an internal standard for the lattice parameter measurements. The lattice parameters were calculated using the computer program *PARA 1* [16], which uses the $\sin^2/\cos^2$ extrapolation model for the hexagonal crystal system.

Results and Discussion

Phase Analysis

The X-ray diffraction scans revealed that the HAp gradually decomposed to tricalcium phosphate $Ca_3(PO_4)_2$ in the presence of increasing silicon concentrations according to the reaction:

$$Ca_{10}(PO_4)_6(OH_2) \longrightarrow 3Ca_3(PO_4)_2 + CaO + H_2O\uparrow$$

Previous studies have shown that SiO_2 can induce the HAp → TCP decomposition [17-19], although none has addressed the case of silicon as the sole additive in an air atmosphere. These studies have investigated the presence of three additives – SiO_2, Al_2O_3, and C in combination – in air [19] or under hydrothermal conditions [17,18]. TCP is an undesirable phase since it is biodegradable *in-vivo* [20].

In the present work, both α- and β-TCP were formed, although β-TCP was favoured at low silicon levels and α-TCP was favoured at higher silicon levels. Further, at higher silicon concentrations, a broad X-ray diffraction peak with a *d* spacing of 0.16-0.26 nm formed. Since both silicon and phosphorus are oxide glass formers, this peak is likely to result from the presence of a Si-P-O glass. For progressively higher silicon levels, the glass became the dominant phase. At very high dopant levels, approximate area ratios of the main diffraction peaks of HAp and TCP suggested that the TCP content was slightly greater than the HAp content.

Traces of the calcium silicophosphate phase $Ca_{10}(PO_4)_4(SiO_4)_2$ appeared at the lowest silicon addition level, and the amount of this phase increased with increasing silicon levels up to the saturation Si:HAp molar ratio of ~0.36. At this point, the main diffraction peak area ratios indicated that the concentration of this phase was similar to that of HAp. This ratio underwent little change at higher silicon addition levels. The appearance of this phase corresponds to the reaction:

$$Ca_{10}(PO_4)_6(OH)_2 + 2Si^{4+} \longrightarrow Ca_{10}(PO_4)_4(SiO_4)_2 + 2P^{5+} + 2OH^-$$

A recent EDS study of SiO_2/HAp mixtures has confirmed that the dissolution of silicon in HAp occurs at a temperature of 1000°C or greater [21].

Variation in the lattice parameters of the HAp with respect to silicon content was measured up to a Si:HAp substitution ratio of 6.94. Beyond this, the HAp diffraction peaks were too depleted by the excessive silicon levels to be measured with any degree of certainty. However, the silicon saturation level, after which the increase in lattice parameters levelled off to a large degree, was graphically estimated to occur at a Si:HAp ratio of ~0.36. Over the range 0-0.36, the following linear lattice expansions were observed:

a = 0.939 to 0.955 nm
c = 0.686 to 0.703 nm for $Ca_{10}(P_6O_{24})(OH)_2$ to $Ca_{10}(P_{5.64}Si_{0.36}O_{24})(OH)_{1.64}$

The data for the corresponding to the unit cell volume expansion are shown in Figure 4.

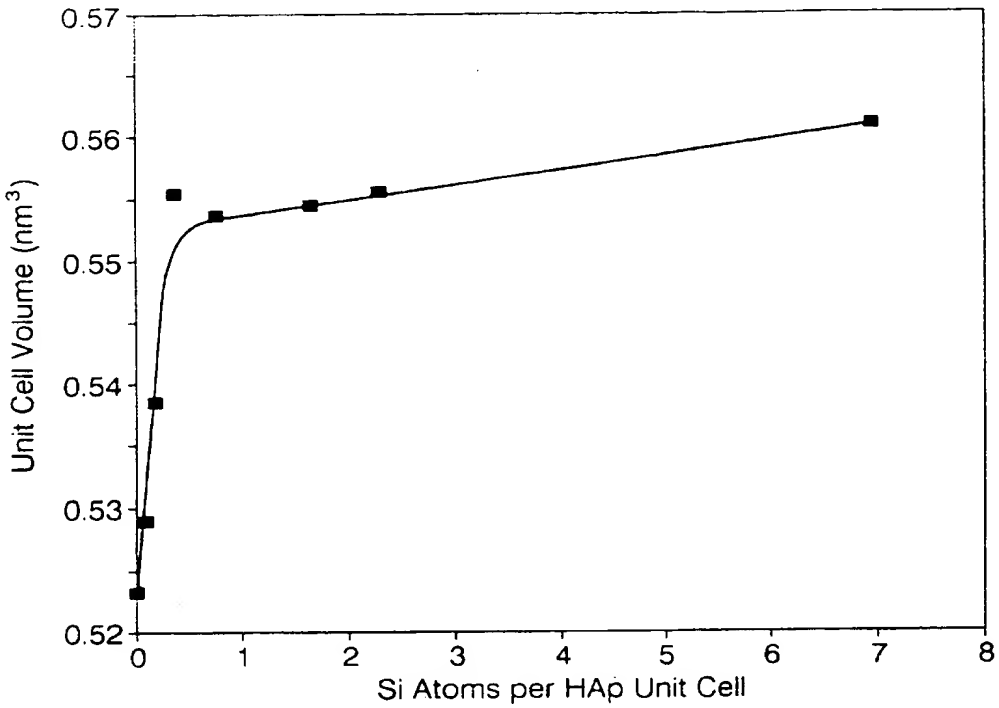

FIGURE 4. UNIT CELL VOLUME EXPANSION OF HAP OWING TO SILICON DISSOLUTION.

The lattice parameters of the undoped HAp measured in the present work are in good agreement with the published literature values, which are a = 0.941 nm [14] or 0.942 nm [22]; c = 0.688 nm [14,22].

The HAp lattice underwent silicon substitution to a saturation level of ~0.36 atoms per unit cell. The substitution site in the $A_{10}(XO_4)_6Z_2$ apatite structure probably was the X site since this site accepts ions within the radius range 0.026-0.056 nm in fourfold coordination [13]. The ionic radius of P^{5+}, the original ion in the X site, is 0.031 nm in fourfold coordination, while Si^{4+} is 0.040 nm•in fourfold coordination [23].

The effect on the lattice parameters of substituting a larger ion into the X site would be an increase in the a and c axes, with $\delta a/\delta c \cong 2$ [24]. In the present work, $\delta a/\delta c$ was significantly lower at ~1. This probably was due to hole formation and partial loss of OH^- ions from the Z sites owing to charge compensation requirements. This would serve to reduce the unit cell volume. The effect on the lattice parameters of depletion of the Z sites would be the opposite of the effect of substitution of larger ions on the Z sites, as reported by Simpson [25]. In the former case, there would be a large decrease in a and a small increase in c.

Combination of the effects of expansion in the X site, giving $\delta a/\delta c \cong 2$, and contraction in the Z site, giving a large and negative δa but a small and positive δc, should result in significant δa and δc values. However, the $\delta a/\delta c$ value would be very difficult to predict reliably. Thus, the present finding of $\delta a/\delta c \cong 0.8$ does not confirm the literature value [24], nor does it contradict it.

The reasons for the relatively low saturation level of silicon in HAp of ~0.36, probably stem from the lattice destabilising effect of the charge imbalance induced by replacing pentavalent P^{5+} with tetravalent Si^{4+}. This charge imbalance was probably compensated by the loss of the weakly held OH^- ions in the Z site. If a sufficient number OH^- ions are lost, structural collapse and the concomitant HAp → TCP transition can result. The Si:HAp substitution limit of ~0.36 may have been a kinetic effect resulting from the relatively short heat treatment time of 1 h, resulting in the retention of the phase $Ca_{10}(P_{0.94}Si_{0.06}O_4)_6(OH)_{1.64}$ [$Ca_{10}(P_{1-X}Si_XO_4)_6(OH)_{2-6X}$, where X = 0.06], in the case of charge compensation. If no charge compensation by OH^- loss occurred, then the phase could be described as $Ca_{10}(P_{1-X}Si_XO_4)_6(OH)_2^{6X-}$, where X = 0.06. The limit of ~0.36 also may have been a result of structural stability limitations.

Conclusions

Doping of HAp by silicon using a sol-gel process resulted in isomorphous substitution of silicon, which probably entered the phosphorous sites in HAp, producing four products:

Calcium Silicophosphate:	$Ca_{10}(PO_4)_4(SiO_4)_2$
Tricalcium Phosphate:	$Ca_3(PO_4)_2$ (significant for Si:HAp > 0.36)
	α-$Ca_3(PO_4)_2$ at higher Si levels
	β-$Ca_3(PO_4)_2$ at lower Si levels
Silicon-Doped HAp:	$Ca_{10}(P_{1-X}Si_XO_4)_6(OH)_{2-6X}$ or
	$Ca_{10}(P_{1-X}Si_XO_4)_6(OH)_2^{6X-}$, where X = 0.06
Si-P-O Glass:	Present at higher Si levels

Therefore, it has been found to be feasible to dope HAp by silicon using a sol-gel route, thereby allowing the future assessment of the effects of silicon on the bioactivity of HAp through clinical trials. However, only low dopant levels should be used in order to maintain the TCP content to a minimum and so eliminate the possibility of biodegradability *in-vivo*. These molar ratio levels are Si:HAp = 0.36:1 and Si:P = 0.06:0.94.

Acknowledgements

The author gratefully acknowledges the assistance of Dr B.J. Baggaley in the quantitative X-ray diffraction analyses and the late Assoc. Prof. E.R. McCartney for helpful discussions.

References

[1] E.M. Carlisle, Nutr. Rev., **40** (1982) 193.
[2] E.M. Carlisle, Calcif. Tissue Int., **33** (1981) 27.
[3] F.H. Nielsen, Ann. Rev. Nutr., **4** (1984) 21.
[4] R.E. Olson and A.A. Doisy, Nutr. Rev., **38** (1980) 194.
[5] E.M. Carlisle, J. Nutr., **110** (1980) 352.

[6] E.M. Carlisle, p. 69 in *Silicon and Siliceous Structures in Biological Systems*. Eds T.L. Simpson and B.E. Volcani. Springer-Verlag, New York, 1981.
[7] W.J. Landis, D.D. Lee, J.T. Brenna, S. Chandra, and G.H. Morrison, Calcif. Tissue Int., **38** (1986) 52.
[8] J.J. Damen and J.M. Ten Cate, J. Dent. Res., **68** (1989) 1355.
[9] J.J. Damen and J.M. Ten Cate, J. Dent. Res., **71** (1992) 453.
[10] P. Li and F. Zhang, Boli Yu Tangci, **16** (1988) 8.
[11] R. Li, Diss. Abs. Int., **B52** (1992) 233.
[12] L.L. Hench, J. Amer. Ceram. Soc., **74** (1991) 1487.
[13] A.G. Cockbain, Miner. Mag., **36** (1968) 654.
[14] C.A. Beevers and D.B. McIntyre, Miner. Mag., **27** (1945) 254.
[15] M. Jarcho, C.H. Bolen, M.B. Thomas, J. Bobick, J.F. Kay, and R.H. Doremus, J. Mater. Sci., **11** (1976) 2027.
[16] B.K. Damkroger, University of New South Wales, School of Materials Science and Engineering, Private Communication.
[17] M.A. Veiderma, Tr. Tallinsk. Politekhn. Inst., Ser. A, **228** (1965) 41.
[18] H. Monma and T. Kanazawa, Bull. Chem. Soc. Japan, **48** (1975) 1816.
[19] E.E. Pomoshchnikov, G.I. Gordeeva, and Y.P. Nikolskaya, Sib. Chem. J., [6] (1973) 109.
[20] S.R. Radin and P. Ducheyne, J. Mater. Sci. Mater. Med., **3** (1992) 33.
[21] K.A. Zeigler, A.J. Ruys, C.C. Sorrell and B.K. Milthorpe, p. 623 in *Ceramics: Adding the Value, Volume 2*. Ed. M.J. Bannister. CSIRO, Melbourne, 1992.
[22] K. Ioku, Y. Masahiro, and S. Somiya, p. 1308 in *Sintering '87, Volume 2*. Eds S. Somiya, M. Shimada, M. Yoshimura, and R. Watanabe. Elsevier, London, 1988.
[23] O. Muller and R. Roy, *The Major Ternary Structural Families*. Springer-Verlag, Berlin, 1974.
[24] D. McConnell, Amer. Mineralog., **22** (1937) 977.
[25] D.R. Simpson, **53** (1968) 432.